Crystals **2014**, *4*, 123-140; doi:10.3390/cryst4020123

OPEN ACCESS

crystals

ISSN 2073-4352

www.mdpi.com/journal/crystals

Article

From Evaporative to Cooling Crystallisation: An Initial Co-Crystallisation Study of Cytosine and Its Fluorinated Derivative with 4-chloro-3,5-dinitrobenzoic Acid

Kate Wittering [1,2], Josh King [1], Lynne H. Thomas [1] and Chick C. Wilson [1,2,*]

[1] Department of Chemistry, University of Bath, Bath, BA2 7AY, UK;
E-Mails: k.wittering@bath.ac.uk (K.W.); joshledleyking@googlemail.com (J.K.);
L.H.Thomas@bath.ac.uk (L.H.T.)

[2] Engineering and Physical Sciences Research Council (EPSRC) Centre for Continuous Manufacturing and Crystallisation (CMAC), University of Bath, Bath, BA2 7AY, UK

* Author to whom correspondence should be addressed; E-Mail: C.C.Wilson@bath.ac.uk;
Tel.: +44-1225-386143; Fax: +44-1225-386231.

Received: 20 December 2013; in revised form: 21 May 2014 / Accepted: 29 May 2014 / Published: 11 June 2014

Abstract: Two new multi-component molecular complexes of cytosine and 5-fluorocytosine with 4-chloro-3,5-dinitrobenzoic acid are presented. Materials synthesis was achieved initially by evaporative crystallisation and the crystal structures determined. The process was then successfully transferred into a controlled small scale cooling crystallisation environment, with bulk samples shown to be representative of the multi-component product phase, by powder X-ray diffraction (PXRD) and differential scanning calorimetry (DSC) methods. Turbidity measurements are shown to be a valuable process analytical technology probe for characterising the initial stages of molecular complex formation in solution. The significance of these findings for scale-up of crystallisation of multi-component molecular materials and for future transfer into continuous cooling crystallisation is discussed.

Keywords: molecular complexes; multi-component crystallisation; continuous manufacturing and crystallisation; cooling crystallisation; process analytical technologies; turbidity measurements

---

1. Introduction

Through manipulation of favourable non-covalent intermolecular interactions between molecular species, crystal engineering can impart or tune a desired physical or chemical property to a material [1]. One important aspect of this method involves multi-component crystallisation, whereby two or more molecular species are crystallised to co-exist within the same crystalline lattice to forming a molecular complex; this could be a salt, co-crystal or solvate. The translation of such multi-component crystallisation into non-evaporative routes is an under-investigated area, and is important to establish if these systems are to be exploited in a range of more industrially-relevant, scalable, crystallisation environments. The initial translation of a multi-component crystallisation system into the cooling environment is one of the important steps in this, offering the potential for further translation towards continuous crystallisation.

The introduction of a second species (also known as a co-former molecule) can significantly alter the physical properties of an active ingredient including, for example, melting point, solubility, stability, compaction and others that may be relevant to the application of the material. Nucleobases are precursors for a range of active pharmaceutical ingredients (APIs) especially cytosine which forms the basis of several anticancer and retroviral drugs such as Lamivudine and Cytarabine [2]. 5-flurocytosine is an antimycotic API that displays anti-fungal properties and is often used for fungal infection treatment administered in combination with amphotericin B [3].

Multi-component crystallisation is commonly carried out using evaporative crystallisation techniques, a particularly facile method of obtaining new crystalline materials [4], but reproducibility and homogeneity can prove difficult due to a lack of control over crystallisation conditions. Alternative methods of crystallisation such as anti-solvent crystallisation and cooling crystallisation can provide more control. Cooling crystallisation is the current method of choice for industrial crystallisation of pharmaceuticals, using large stirred tank reactors (STRs) in a batch workflow. This has been the "workhorse" of industrial crystallisation for the past 100 years [5]. In an attempt to revolutionise this process the EPSRC Centre for Continuous Manufacturing and Crystallisation (CMAC), a multidisciplinary centre based on an academic-industrial partnership including seven institutions in the UK, is focused upon developing the scientific and technical basis for transferring industrial crystallisation from a batch to a continuous process.

The majority of continuous crystallisation technologies, which include the continuous oscillatory baffled crystalliser (COBC) [6] and the Rattlesnake continuous crystallizer [7], operate via cooling crystallisation and thus the first step in transfer of multi-component crystallisation towards a continuous process is to convert from small scale evaporation processes into cooling crystallisation; it is this initial step that is targeted in this work. Many studies have been reported on the control of cooling crystallisation of single component materials [8,9]; however, control of a crystallisation process is made significantly more complex by the addition of a co-former where there can be significant differences in the relative solubilities of the two (or more) components; to improve solubility, co-formers are often chosen to be much more soluble than the target material [4]. In addition, in some cases the solubility of the components can be affected by the presence of the other molecules in the multi-component solution.

Initial solubility measurements using process analytical tools (PAT), including turbidity probes and UV/Vis probes, can indicate the differences in solubility between the co-former and the target. This is important both in inducing solubility as a target property in itself and also to inform design of the crystallisation process. To overcome the disparity in component solubilities, the stoichiometry of starting materials can be altered so that a higher percentage of the more soluble material is added to solution, although in some cases this may have an unwanted effect upon the stoichiometry within the multi-component molecular complex. In addition to this, a combination of solvents can be used in varied ratios to help increase the likelihood of crystallising the desired multi-component molecular complex rather than the starting materials or any other unwanted by-products. The possible occurrence of impurities, polymorphs of starting materials, hydrates and/or solvates and alternative polymorphs of multi-component molecular complexes can rapidly increase the complexity of the crystallisation process.

It is common to identify the metastable zone width (MSZW) to establish the boundaries of the crystallisation space within which the solution is supersaturated but not labile, *i.e.*, spontaneous nucleation does not occur rapidly [10,11]. The MSZW can be defined as the variation in temperature between the point of saturation and the point at which crystal nucleation occurs (or is detected). It can prove particularly challenging to determine the MSZW of a multi-component material, especially if the system is polymorphic, as it is difficult to obtain phase pure multi-component material with no impurities or residual starting materials that may complicate the analysis.

The study reported here targets interactions between the nucleobases, cytosine and 5-fluorocytosine, and the carboxylic acid group of 4-chloro-3,5-dinitrobenzoic acid; the controlled production of multi-component molecular complexes through modification of crystallisation methods is investigated. The two new molecular complexes produced in this study were selected as candidates for scale up to continuous crystallisation. This report details the preliminary experiments to transfer these systems into controlled small scale cooling crystallisation, as a first step towards developing a route to continuous crystallisation of these systems.

2. Results and Discussion

2.1. Molecular Complexes of Cytosine and 5-Fluorocytosine with 4-chloro-3,5-Dinitrobenzoic Acid

Two new multi-component molecular complexes were synthesised through evaporative crystallisation studies involving cytosine, 5-fluorocytosine (5FC) and 4-chloro-3,5-dinitrobenzoic acid (4Cl35DNBA). Sample preparation and crystallographic data collection details are given in the experimental section.

The 1:1 molecular complex of 5-fluorocytosine and 4-chloro-3,5-dinitrobenzoic acid (5FC-4Cl35DNBA) is a salt with proton transfer indicated from the carboxylic acid group of 4Cl35DNBA to the lone pair of the free N2 of 5FC. Heterodimers are formed through two charge-assisted N–H···O hydrogen bonds (N···O distances 2.722(1) Å and 2.803(1) Å) (Figure 1a,b). Two heterodimers related by a centre of inversion combine to form a tetramer through an additional N–H···O hydrogen bond (N···O 2.871(1) Å) as well as a C–H···F weak hydrogen bond (C···F 3.091(1) Å). Each tetramer unit forms two further hydrogen bonds to neighbouring tetramers through atoms O6 (H-bond acceptor) and N1 (H-bond donor). These connected chains pack in a zig-zag, layered arrangement along the −1 0 1 plane.

Figure 1. A tetramer unit of the 5FC-4Cl35DNBA molecular complex. (**a**) and (**b**) are the N–H···O hydrogen bonds forming the dimer; (**c**) and (**d**) are the N–H···O and C–H···F hydrogen bonds, respectively, that connect the two dimers together into the tetramer.

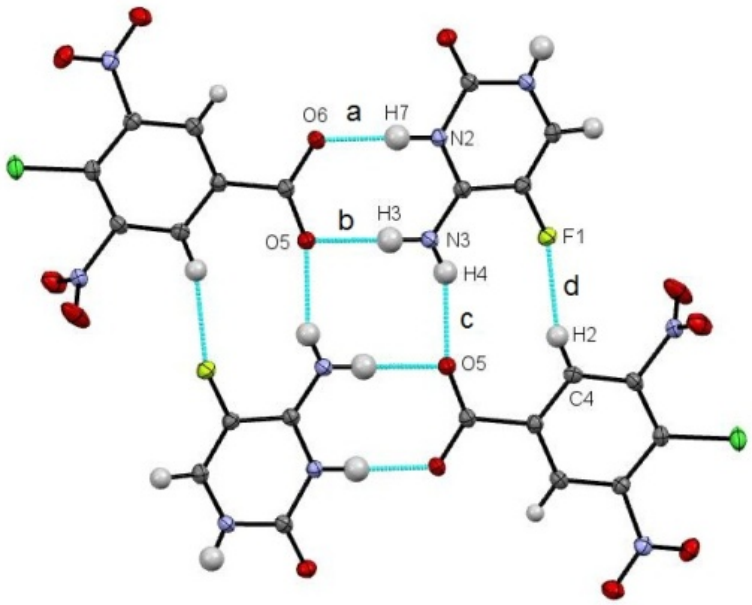

Powder X-ray diffraction (PXRD) shows that when crystallisation is initiated from a solution of a 1:1 ratio or a 2:1 ratio of starting materials (5FC:4Cl35DNBA), the same 1:1 5FC-4Cl35DNBA complex is formed, which is indicated by the intense peaks at 24.4° 2θ and 27.3° 2θ in the PXRD (Figure 2). However, when crystallised using a 1:2 starting ratio of 5FC to 4Cl35DNBA a unique and intense PXRD peak can be seen at 26.4° 2θ. This does not correspond to the 5FC-4Cl35DNBA complex, nor is it representative of either 5FC or 4Cl35DNBA (including any known hydrates or solvates). This would infer that there is new material present, which could be a new polymorph, a new multi-component molecular complex or another solvate of the starting materials; further analysis is required to elucidate this phase.

Differential scanning calorimetry (DSC) of a pure sample of 5FC-4Cl35DNBA arising from 1:1 evaporative crystallisation (as characterised through PXRD) shows a single endothermic event at 196.1 °C prior to decomposition (Figure 3a). This does not correspond to the DSC traces of the 4Cl35DNBA and 5FC starting materials. 4Cl35DNBA displays an endothermic event at 162.2 °C (Figure 3b), which corresponds to its literature melting point of 159–162 °C and 5FC displays an exothermic event at 292.6 °C, which corresponds to 5FC thermal decomposition (296 °C) (Figure 3c).

In contrast to the 5FC-4Cl35DNBA molecular complex, cytosine (CYT) forms a monohydrated 2:1 complex with 4Cl35DNBA (CYT-4Cl35DNBA). The asymmetric unit contains a water molecule, a single 4Cl35DNBA molecule and two cytosine molecules (Figure 4). Interestingly, only one cytosine molecule remains neutral while the other accepts a proton from the carboxylic acid group of the 4Cl35DNBA molecule. De-protonation of the carboxylic acid group is indicated by the similarities in the C8–O3 and C8–O4 bond distances, at 1.230(3) Å and 1.258(3) Å, respectively.

Figure 2. (**a**) PXRD pattern generated from the single crystal determined structure of 5FC-4Cl35DNBA for comparison with PXRD patterns of (**b**) 4Cl35DNBA; (**c**) 5FC; and products of evaporative crystallisation of 5FC: 4Cl35DNBA in various ratios: (**d**) 1:2; (**e**) 2:1; and (**f**) 1:1 (all crystallisations in ethanol and water 1:1 by volume).

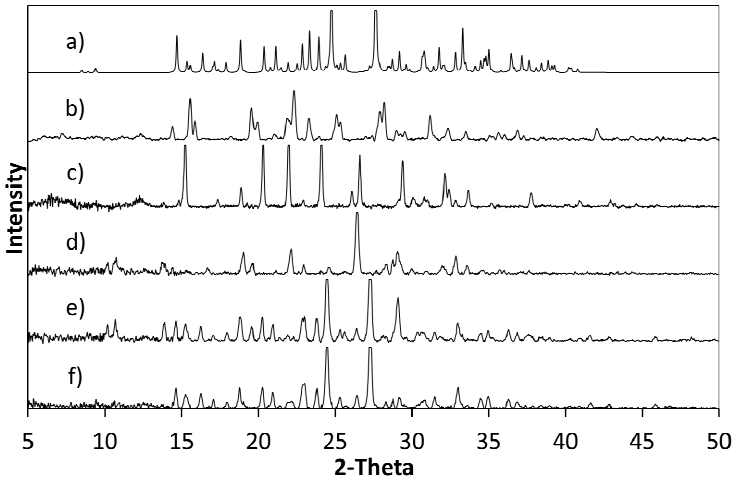

Figure 3. Differential scanning calorimetry of (**a**) 5FC-4Cl35DNBA; (**b**) 4Cl35DNBA; (**c**) 5FC.

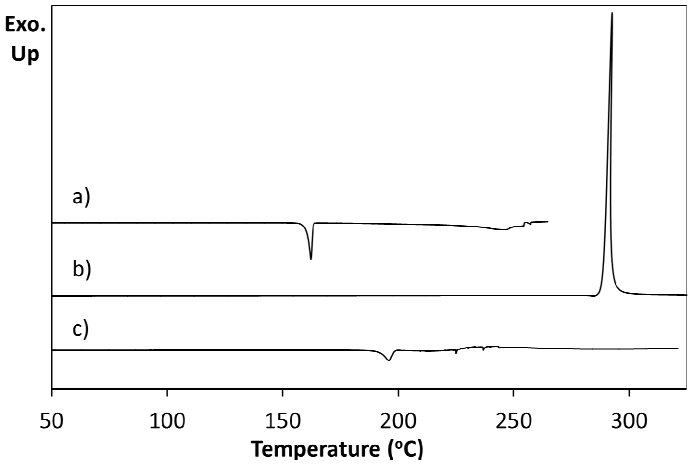

Figure 4. Asymmetric unit of CYT-4Cl35DNBA displaying the hydrogen bonding interactions of the deprotonated 4Cl35DNBA carboxylic acid group with the cytosine homodimer.

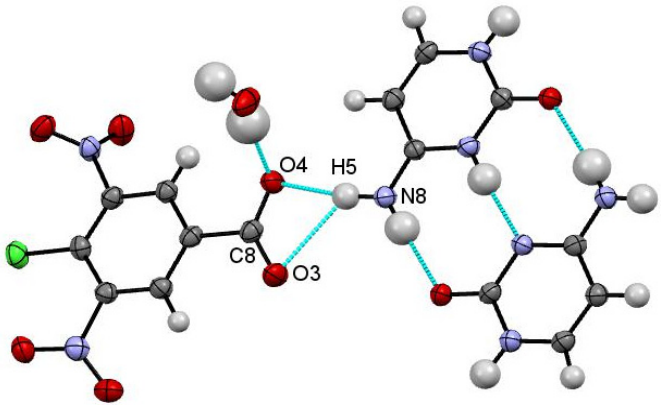

Variation in the protonation states of the two cytosine species facilitates formation of a cytosine homodimer bound through a pseudo Watson-Crick hydrogen bonding interaction consisting of three moderately strong hydrogen bonds N8–H6···O17, N9–H4···N16 and N14–H13···O13 with D···A distances of 2.809 (3) Å, 2.820 (3) Å and 2.865 (3) Å, respectively (Figure 5). Three further prominent hydrogen bonds link the three components of the molecular complex, and are also shown in Figure 4. Atom H5 acts as a bifurcated hydrogen bond donor to the carboxylate ion of 4Cl35DNBA and the water molecule forms a moderate strength hydrogen bond with atom O4 of the carboxylate group. The cytosine and 4Cl35DNBA molecules lie parallel to the 1 0 −1 plane, with each of the inversion related layers hydrogen bonding to another through a water molecule.

Figure 5. A cytosine dimer with pseudo Watson-Crick hydrogen bonding arrangement within CYT-4Cl35DNBA.

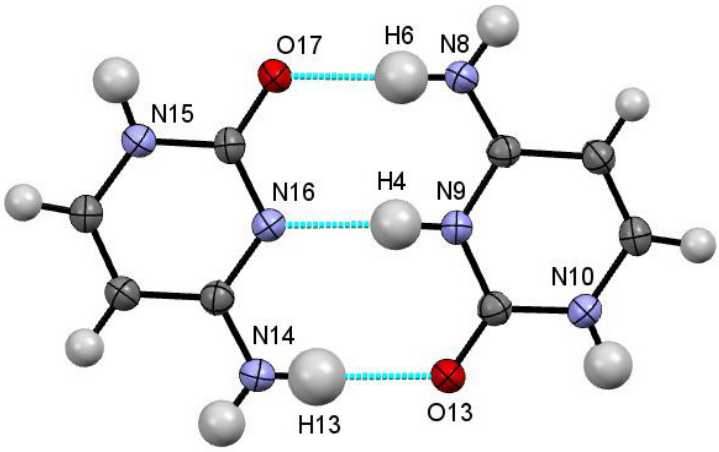

The products of further evaporative crystallisations of cytosine with 4Cl35DNBA were analysed using a combination of single crystal X-ray diffraction (SXRD) and PXRD (Figure 6). This confirmed that when using a 2:1 ratio of cytosine to 4Cl35DNBA the initial stoichiometry was retained and the 2:1 molecular complex CYT-4Cl35DNBA was produced. However, when a 1:1 stoichiometry of starting materials was used a crystalline powder was formed and the resulting PXRD pattern does not correspond to any of the starting materials (including polymorphs or solvates) or to the 2:1 molecular complex; it may, therefore, represent an additional unknown complex which could be a 1:1 molecular complex of cytosine and 4Cl35DNBA or a non-hydrated molecular complex of cytosine and 4Cl35DNBA. The DSC trace for this form is simpler than that observed for the 2:1 CYT-4Cl35DNBA a single endothermic event at a similar onset temperature to the second event in the 2:1 molecular complex (1:1, 192.3 °C; 2:1 184.2 °C) (Figure 7). The DSC trace for the 2:1 complex has an initial broad endothermic event at 95 °C which may reflect a desolvation process or a transformation into a different polymorphic or stoichiometric form.

Figure 6. PXRD patterns of (**a**) cytosine; (**b**) 4Cl35DNBA and (**c**) a pattern calculated from the single crystal structure of CYT-4Cl35DNBA. These were compared with PXRD patterns of bulk products of evaporative crystallisation of cytosine and 4Cl35DNBA from different crystallisation conditions using (**d**) a 2:1 starting material ratio from ethanol and water (1:1 by volume); (**e**) a 1:1 starting material ratio from acetone and water (1:1 by volume); (**f**) a 2:1 starting material ratio in acetone and water (1:1 by volume) and (**g**) supersaturated preparation from which the single crystal used for full SXRD data was obtained.

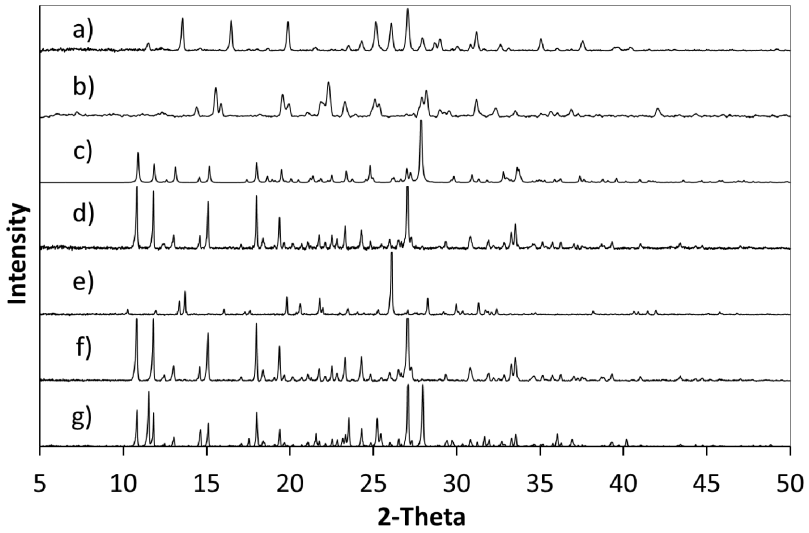

Figure 7. Differential scanning calorimetry of (**a**) 4Cl35DNBA and (**b**) cytosine, together with those for products of the evaporative crystallisation of cytosine and 4ClDNBA in: (**c**) a 2:1 starting material ratio in ethanol and water (1:1 by volume); (**d**) a 2:1 starting material ratio in acetone and water (1:1 by volume); (**e**) a 1:1 starting material ratio in acetone and water (1:1 by volume).

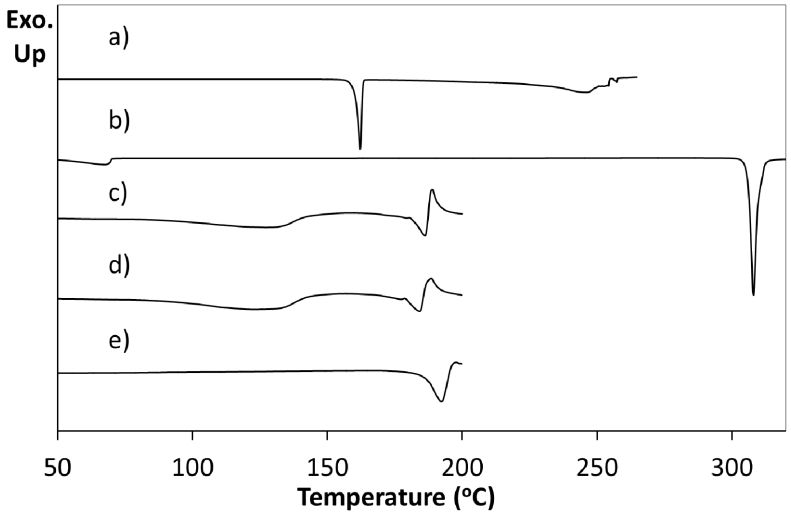

2.2. New Polymorphic Form of Starting Material, 4Cl35DNBA Form II

Further to the discovery of two new multi-component molecular complexes, an additional polymorphic form (Form II) of the starting material 4Cl35DNBA (Form II) was characterised. The known crystal structure of 4Cl35DNBA (Form I) (Cambridge Structural Database (CSD) Refcode TIBGIV) contains one molecule in the asymmetric unit and crystallises in the triclinic crystal system with space group P-1 [12]. The PXRD pattern of the 4Cl35DNBA starting material taken as received from Sigma Aldrich does not match the PXRD pattern generated from SXRD data of Form I (Figure 8). The asymmetric unit of Form II consists of two independent 4Cl35DNBA molecules connected through two O–H···O hydrogen bonds between the carboxylic acid moieties creating a carboxylic acid dimer motif. Form I also contains similar 4Cl35DNBA homodimer motifs; however, the homodimeric motif in Form I is planar in contrast to the twisted, non-planar dimer of Form II (Figure 9). In both polymorphs the homodimers pack through π–π stacking interactions to form sheets but with differing staggering of the homodimer units (Figure 10).

Figure 8. PXRD patterns of (**a**) 4Cl35DNBA Form I (calculated from SXRD structure); (**b**) 4Cl35DNBA Form II (calculated); (**c**) 4Cl35DNBA Form II (as supplied from Sigma Aldrich).

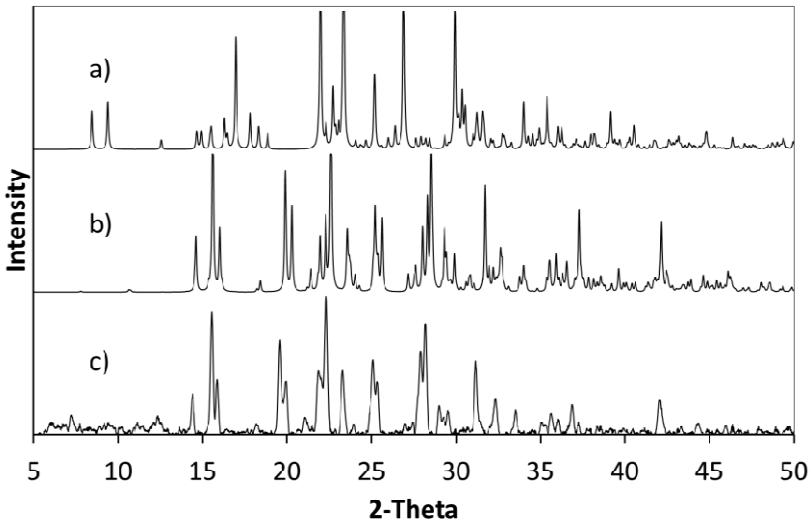

Figure 9. Hydrogen bonded dimer of 4Cl35DNBA in: (**a**) 4Cl35DNBA Form I; (**b**) 4Cl35DNBA Form II.

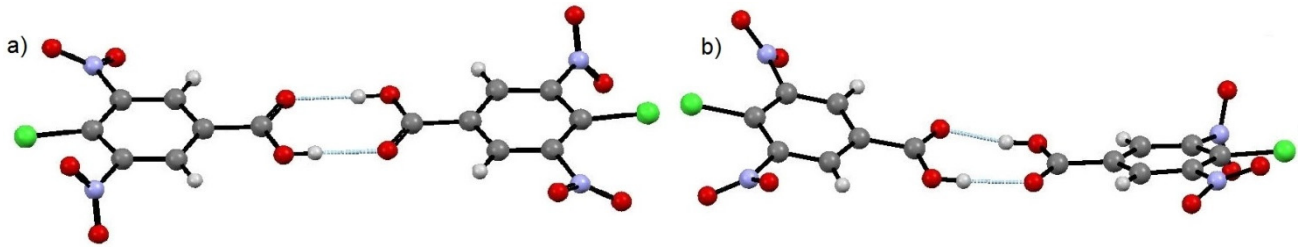

Figure 10. 4Cl35DNBA dimers packing into layered sheets through π–π stacking interactions in: (**a**) 4Cl35DNBA Form I; (**b**) 4Cl35DNBA Form II.

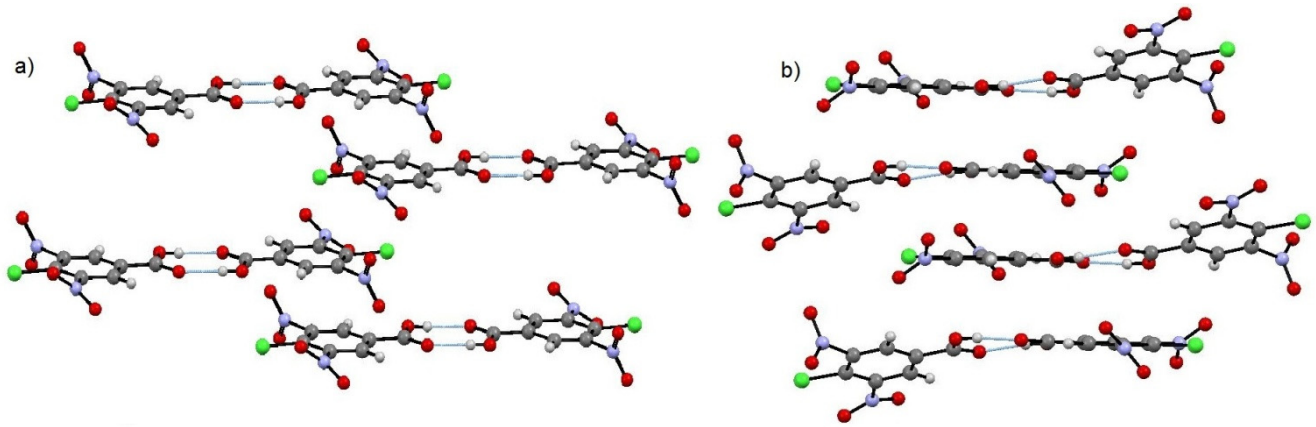

2.3. Solubility Measurements of 5FC-4Cl35DNBA

To inform and help interpret the targeted cooling crystallisation experiments, and also as a key target property in crystal engineering approaches to new solid forms, solubility analysis of 5FC-4Cl35DNBA was carried out using the Crystal16 and confirms that the molecular complex is significantly more insoluble that both 5FC and 4Cl35DNBA starting materials (Figure 11). It proved difficult to collect a wide range of solubility data for 4Cl35DNBA using the Crystal16 due to its very high solubility. The volume of solid required to saturate the solution at high temperatures was too great for the small 2 mL vials. Additionally, when using large volumes of solid magnetic stirring within the vials was hindered.

Figure 11. Comparison of solubility of 5FC-4Cl35DNBA co-crystal with 5FC and 4Cl35DNBA starting materials.

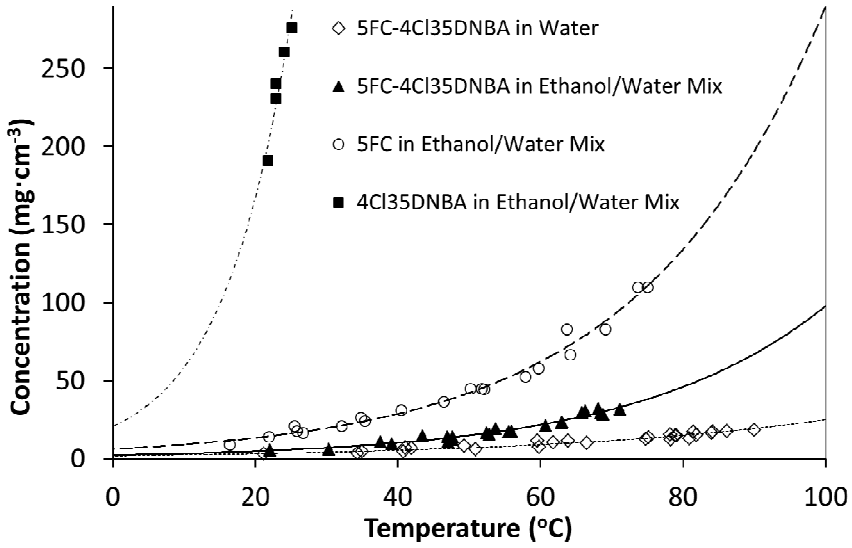

2.4. Translation into Cooling Crystallisation

Four cooling crystallisations of 4Cl35DNBA with cytosine or 5FC with differing conditions (Table 1); all produced very fine, yellow needle crystals. SXRD analysis of each sample showed that several crystals in each preparation corresponded to the targeted molecular complex previously discovered through evaporative routes as described above.

Table 1. Conditions of cooling crystallisations using a ReactArray Reaction Block.

Sample	Components	Ratio	Solvent	Solvent Ratio	Cooling profile
A	cytosine, 4Cl35DNBA	1:1	acetone and water	1:1	1
B	5FC, 4Cl35DNBA	1:1	acetone and water	1:1	1
C	5FC, 4Cl35DNBA	1:1	ethanol and water	1:1	2
D	5FC, 4Cl35DNBA	1:2	ethanol and water	1:1	2

PXRD analysis of sample A (Figure 12) confirmed that CYT-4Cl35DNBA was produced, though it is important to note that the peak intensities do vary due to preferred orientation. The bulk of samples B, C and D were confirmed to be 5FC-4Cl35DNBA (Figure 13).

Solubility analysis showed 4Cl35DNBA to be approximately six times more soluble in ethanol than 5FC. 5FC was more soluble in ethanol than in water and 4Cl35DNBA did not dissolve in water alone. In light of this a mixture of ethanol and water was used to help to reduce the solubility of 4Cl35DNBA. Turbidity measurements showed a 7:3 mixture of ethanol to water (by volume) to be a suitable ratio of solvents for this system.

Figure 12. PXRD analysis of product of cooling crystallisation A. The plot compares the PXRD patterns for starting materials: (**a**) CYT; (**b**) 4Cl35DNBA, and the PXRD pattern for (**c**) CYT-4Cl35DNBA calculated from single crystal data with that of (**d**) Product A. The peak positions show that A contains the same CYT-4Cl35DNBA complex as found in the 2:1 evaporative experiment, though the intensities are heavily affected by preferred orientation.

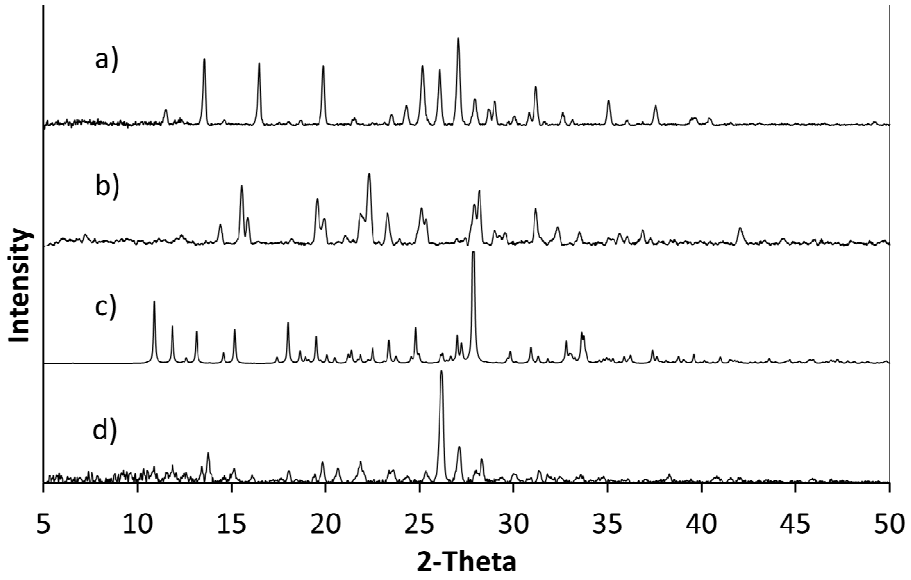

Figure 13. PXRD analysis of cooling crystallisations B, C and D. (**a**) 5FC; (**b**) 4Cl35DNBA; (**c**) 5FC-4Cl35DNBA; (**d**) Product B; (**e**) Product C; (**f**) Product D.

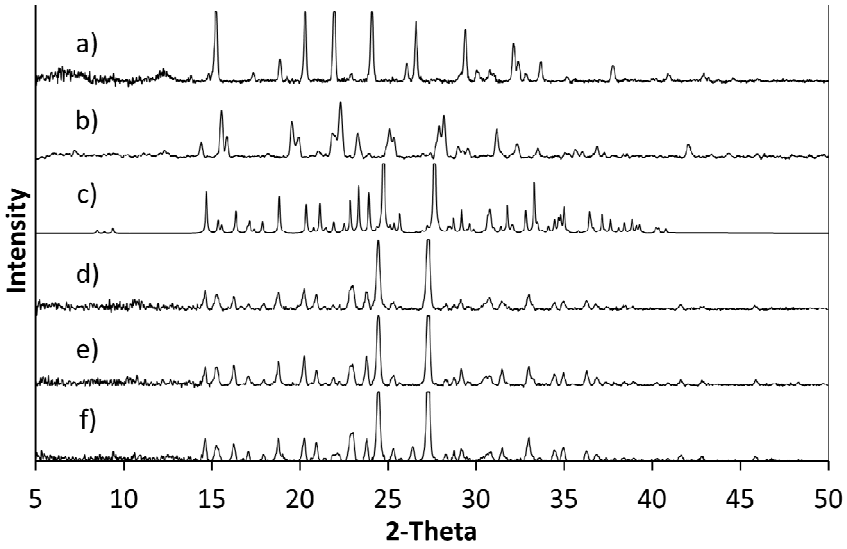

The formation of 5FC-4CL35DNBA could be followed during the cooling crystallisation using turbidimetric methods using a Crystal16 apparatus (Figure 14). Initially the turbidity signal is noisy due to the particle size but ranges from 60% to 100% transmittance. As the temperature increases the solution becomes turbid and the transmittance drops to 0%. This increase in turbidity with an increase in temperature in the early stages of the process is perhaps counterintuitive and indicates the initial, rapid, crystallisation of the less soluble multi-component complex (as shown by previous solubility measurements). As the temperature continues to increase, 5FC-4Cl35DNBA dissolves and the solution develops 100% transmittance. 5FC-4Cl35DNBA then recrystallises upon cooling and the transmittance returns to 0%. Importantly, repetition of the heating and cooling temperature ramps then follows the expected trend, showing cloud points and clear points at the same temperatures as before. It should be noted that there are very few previous examples of the crystallisation of multi-component complexes by cooling at this small scale. This relatively simple methodology thus acts as an exemplar for the intended transfer of such processes into the continuous environment, by establishing the initial cooling stage.

It is also useful to note that these determinations illustrate that significant progress can be made in establishing such crystallisation processes using relatively simple analytical methods such as turbidity measurement. While acknowledging its inherent limitations, it is of value that this can be achieved even in the absence of full process analytical technologies (PAT), which will be implemented in future development of this work.

PXRD analysis of a range of samples from Crystal16 experiments confirm the formation of 5FC-4Cl35DNBA (Figure 15) as indicated by the initial precipitation shown in the turbidity data. It should be noted, however, that when a slower cooling rate of 0.5 °C min^{-1} was used, residual 4Cl35DNBA form II was present in the product as shown by the additional peaks in the PXRD pattern at 15.6° 2θ and 28.2° 2θ (Figure 15d). While such a slow cooling rate is unlikely to be industrially relevant, for example, this element of the study was undertaken to explore the effect of cooling rate on the crystallisation products. The melt at 154.3 °C observed in DSC analysis (Figure 16a) is much lower than those for the other samples, and is similar to the melting point of 4Cl35DNBA form II (162.2 °C).

The other samples show endothermic events at 197.9 °C and 195.8 °C which are consistent with the 5FC-4Cl35DNBA sample produced from evaporative cooling as discussed above.

Figure 14. Turbidity data from cooling crystallisation of 5FC with 4CL35DNBA (1:2) in ethanol and water (7:3 by volume). The temperature regimes used are shown as the red trace.

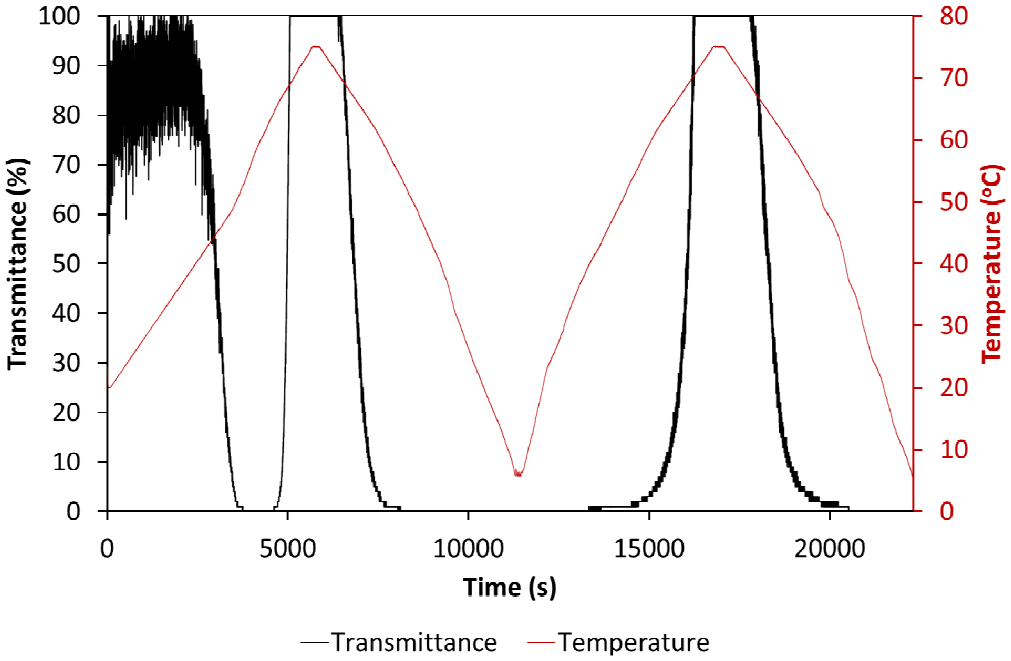

Figure 15. PXRD analysis of cooling crystallisations carried out using the Crystal16 apparatus: (**a**) 5FC; (**b**) 4Cl35DNBA form II; (**c**) 5FC-4Cl35DNBA 5FC:4Cl35DNBA in ethanol:water (7:3 by volume) in (**d**) a 1:2 starting material ratio (0.5 °C min^{-1}); (**e**) a 1:2 starting material ratio (2 °C min^{-1}) and (**f**) a 1:1 starting material ratio (2 °C min^{-1}).

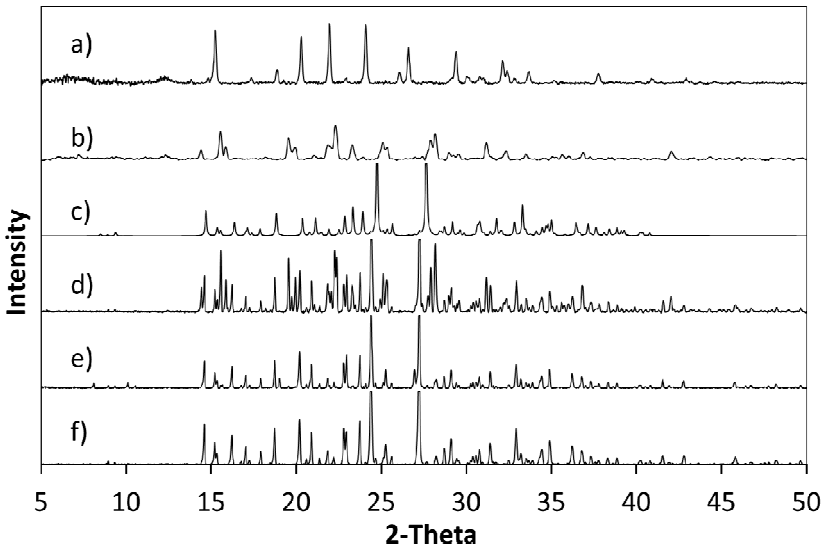

Figure 16. Differential scanning calorimetry of products from cooling crystallisations using the Crystal16 involving 5FC-4Cl35DNBA 5FC:4Cl35DNBA in ethanol:water (7:3 by volume) in a: (**a**) a 1:2 ratio (0.5 °C min^{-1}); (**b**) a 1:2 ratio (2 °C min^{-1}); and (**c**) a 1:1 ratio (2 °C min^{-1}); (**d**) 4Cl35DNBA; (**e**) 5FC.

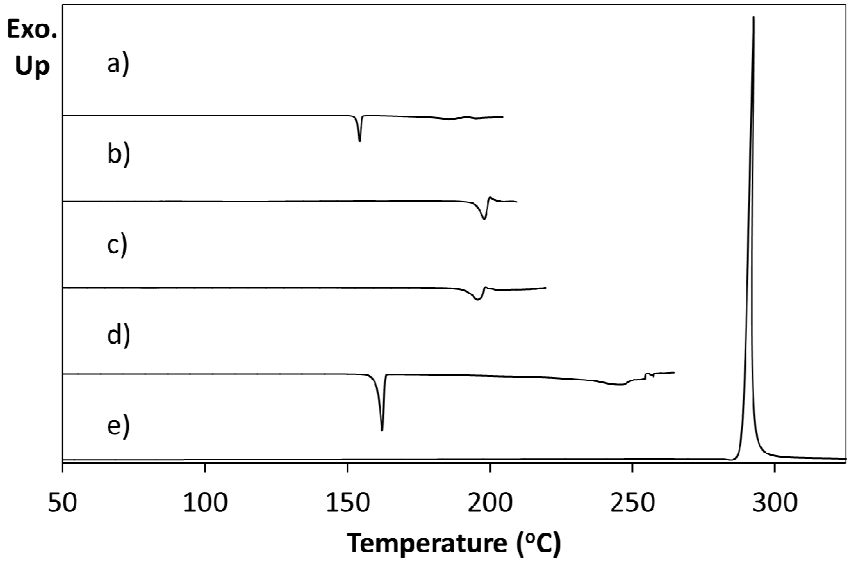

3. Experimental Section

3.1. Materials

All experiments used either 5-fluorocytosine, 98% pure from Fluorochem Ltd. (Hadfield, UK), or cytosine, 99% pure, and 4-chloro-3,5-dinitrobenzoic acid, 97% pure from Sigma Aldrich (Gillingham, UK). Crystallizations were performed using either 99% acetone or 99.8% ethanol from Sigma Aldrich in combination with deionized water.

3.2. Evaporative Crystallisation

3.2.1. 5FC-4Cl35DNBA

5FC and 4Cl35DNBA were co-crystallised in an ethanol and water solvent mix (1:1 by volume). 5FC (13.2 mg) and 4Cl35DNBA (12.9 mg) were measured into a glass vial and dissolved in the solvent solution using a combination of sonication and gentle heating. The solution was added into a single glass vial, sealed with a perforated plastic lid and left at room temperature (18–22 °C) for slow evaporative crystallisation.

3.2.2. CYT-4Cl35DNBA

CYT-4Cl35DNBA was formed from a saturated solution of the molecular components. 20 mL of acetone and water solvent solution (1:1 by volume) was added to a conical flask followed by a 4:1 ratio of cytosine: 4Cl35DNBA until a fully saturated solution was achieved for cooling crystallisation (111.5 mg 4Cl35DNBA and 236.5 mg cytosine). However, this sample immediately formed a slurry which did not settle over time. A small aliquot was transferred into a separate vial where solvent was

allowed to evaporate at a constant temperature of 30 °C. After approximately 24 h, several single crystals formed. These were subsequently used for SXRD analysis. Interestingly, after 48 h, at 30 °C the rest of the slurry suspension began to re-dissolve. After 5–7 days the solvent had completely solvent evaporated and a mixture of small, yellow needle crystals and larger plate crystals were produced.

3.2.3. 4Cl35DNBA Form II

Attempts at co-crystallisation with 5FC and 4Cl35DNBA from ethanol and water (1:1 by volume) via small scale evaporative crystallisation yielded single crystals of 4Cl35DNBA Form II which was shown to be a polymorphic form of the 4Cl35DNBA starting material, as supplied by Sigma Aldrich.

3.3. Cooling Crystallisation: Preliminary Small Scale Studies Using the React Array Reaction Block

Each mixture of molecular components was added to 20 mL of hot solvent solution (50 °C) until saturated. After which the solution was left to settle whilst held at 50 °C. The top aliquot was removed using a heated syringe with micro filter and was subsequently divided into several 2.5 mL glass vials, each sealed with a cap and plastic paraffin film to minimise any possibility of evaporative crystallisation. The glass vials were then placed into a ReactArray Solo Microvate Reaction Block (RB) (Anachem Ltd., Luton, UK) with an RS12 power supply and subjected to one of two cooling profiles generated and controlled using ReactArray Solo software [13]. In cooling profile 1, which was used for solutions prepared with acetone, the vials were held at 50 °C for an hour followed by cooling to −5 °C at 0.2 °C min^{-1}. Cooling profile 2 held the vials at 65 °C for an hour prior to cooling at a rate of 0.5 °C min^{-1} to −5 °C. This was used for solutions prepared with ethanol. Details of the cooling crystallisations using the RB are provided in Table 1 above.

3.4. Analysis

3.4.1. X-ray Diffraction

The single crystal X-ray diffraction data were collected using a Rigaku R-Axis/RAPID image plate diffractometer using graphite monochromated Mo Kα radiation (λ = 0.71073 Å) at a temperature of 100 K. The structures were solved by direct methods using either SHELXS-97 [14] within the WinGX v1.8.05 package [15] or SHELXS-2013 within the WinGX v2013.2 package [16]. All structures were refined using SHELXL-2013, with crystallographic parameters shown in Table 2.

Powder X-ray diffraction data were collected in capillary mode on a Bruker D8 Advance equipped with monochromated Cu Kα radiation (λ = 1.54056 Å) in transmission geometry at 298 K.

3.4.2. Differential Scanning Calorimetry

A TA DSC Q20 with Thermal Advantage Cooling System 90 (TA Instruments, Elstree, UK) was used for differential scanning calorimetry (DSC) studies, using nitrogen gas at a flow rate of 18 cm^3 min^{-1} and a temperature ramp rate of 2 °C min^{-1}. Data were collected using the Advantage for Qseries [17].

Table 2. Crystallographic information on two new multi-component molecular complexes of 4Cl35DNBA and a new polymorphic form of 4Cl35DNBA.

Molecular Complex	5FC-4Cl35DNBA	CYT-4Cl35DNBA	4Cl35DNBA (Form II)
Formula	$[C_4H_5ON_3F]^+$ $[C_7H_2N_2O_6Cl]^-$	$C_4H_5N_3O{\cdot}[C_4H_6N_3O]^+$ $[C_7H_2N_2O_6Cl]^-{\cdot}H_2O$	$C_7H_3ClN_2O_6$
Molecular weight (g mol^{-1})	375.7	486.8	246.6
Temperature (K)	100	100	100
Space group	$P2_1/n$	$P2_1/c$	$P2_1/n$
a (Å)	12.068(1)	14.383(3)	8.9032(4)
b (Å)	6.0558(6)	8.399(2)	8.9201(6)
c (Å)	18.857(2)	17.339(4)	22.697(2)
α (°)	90.00	90.00	90.00
β (°)	93.021(7)	110.478(8)	90.880(6)
γ (°)	90.00	90.00	90.00
Volume (Å^3)	1,376.2(3)	1,962.1(7)	1,802.3(2)
Z	4	4	8
ρ (calcd)/Mg m^{-3}	1.813	1.648	1.817
θ range/°	3.2–27.5	3.0–27.5	3.2–27.5
Completeness	99.9	99.9	99.8
Reflections collected	17,302	24,995	20,452
No. of unique data [R_{int}]	3,153 [0.031]	4,495 [0.096]	4,130 [0.029]
No. of reflections with $I > 2\sigma(I)$	2,918	2,748	3,532
GooF on F^2	1.063	1.004	1.017
Final R_1 ($I > 2\ \sigma(I)$)	0.029	0.052	0.028
Final wR_2 (all data)	0.081	0.152	0.069
CCDC No.	976509	976510	976508

3.4.3. Solubility Measurement

Solubilities of the starting materials in the respective solvent of crystallisation were measured using the Crystal16 parallel crystalliser (Avantium Technologies BV, Amsterdam, The Netherlands). Using turbidity probes the Crystal16 is capable of measuring the clear and cloud points of up to sixteen 1 mL solutions simultaneously. Vials were cycled through temperature ranges from 5 °C to 75 °C using a temperature ramp rate of 0.5 °C min^{-1}, with bottom stirring at 850 rpm using standard magnetic stirrer bars. At the end of the final cycle samples were cooled at a slower rate of 0.1 °C min^{-1} to promote growth of larger crystals. Data were analysed using CrystalClear [18].

4. Conclusions

The work presented here represents the initial attempts to develop control over cooling crystallisation of these multi-component molecular systems. The crystallisation products from evaporative experiments have been reproduced using small scale cooling crystallisation and attempts have been made to optimise the crystallisation conditions to enable full conversion to the co-crystal.

The initial empirical approach reported here should be augmented and supported by more comprehensive quantitative studies, for example using PAT exploiting different spectroscopic probes such as solution state Raman and Infrared spectroscopies, or by comprehensive dissolution studies. In particular further investigation is required to understand fully the initial association process visualised in this work by the simplest of these PAT methods, turbidity. However, this initial, empirical investigation has established crystallisation under cooling of the target complexes, and the dependence of yield of co-crystal as a function of cooling rate. This is of immediate value to the aim of establishing a cooling regime for initial transfer into the cooling/continuous crystallisation environment. The Crystal16 has been used previously to map out phases for multi-component systems [19] and the overarching aim is to carry out full mapping of these systems to aid control of future crystallisation scale up for multi-component systems. This apparatus also shows potential for future insight into the crystallisation kinetics of the multi-component nucleation process through study of MSZW and crystallisation induction times [20].

Understanding, monitoring and control of the initial association step in crystallisation is a key theme within the CMAC collaboration. It provides fundamental underpinning preparation for future scale-up, in order to achieve a well-integrated and controlled cooling crystallisation process with uniform particle attributes in the continuous crystallisation environment [21]. This will be the subject on ongoing work in this area.

Acknowledgments

This work was carried out as part of the EPSRC Centre for Innovative Manufacturing in Continuous Manufacturing and Crystallisation (CMAC), under grant EP/I033459/1. The authors would like to thank Avantium Technologies BV for loan of Crystal16 apparatus to carry out solubility measurements and *in-situ* monitoring and control of multi-component crystallisation. Dyanne Cruickshank is thanked for discussions, and Thomas McGlone and Rajni Miglani Bardwaj (CMAC, University of Strathclyde) for additional PXRD patterns and for access to solubility measurements. Funding from the University of Bath is also acknowledged.

Author Contributions

Kate Wittering carried out experimental work, the majority of the analysis and contributed to writing of the MS; Josh King carried out experimental work and analysis; Lynne H. Thomas co-supervised the research, contributed to crystal structure data collection and analysis and MS writing; Chick C. Wilson led and supervised the research, was involved in experiment design and data analysis and contributed to writing of the MS.

Conflicts of Interest

The authors declare no conflict of interest.

References

1. Desiraju, G.R. Crystal engineering: A brief overview. *J. Chem. Sci.* **2010**, *122*, 667–675.
2. Bhatt, P.M.; Azim, Y.; Thakur, T.S.; Desiraju, G.R. Co-Crystals of the Anti-HIV Drugs Lamivudine and Zidovudine. *Cryst. Growth Des.* **2009**, *9*, 951–957.
3. Vermes, A.; Guchelaar, H.J.; Dankert, J. Flucytosine: A review of its pharmacology, clinical indications, pharmacokinetics, toxicity and drug interactions. *J. Antimicrob. Chemother.* **2000**, *46*, 171–179.
4. Aakeröy, C.B.; Forbes, S.; Desper, J. Using Cocrystals to Systematically Modulate Aqueous Solubility and Melting Behavior of Anticancer Drugs. *J. Am. Chem. Soc.* **2009**, *131*, 17048–17049.
5. Ni, X.-W. Bridging the Gap. *Chem. Eng.* **2008**, *800*, 36–38.
6. Lawton, S.; Steele, G.; Shering, P.; Zhao, L.; Laird, I.; Ni, X.-W. Continuous Crystallization of Pharmaceuticals Using a Continuous Oscillatory Baffled Crystallizer. *Org. Process Res. Dev.* **2009**, *13*, 1357–1363.
7. Cambridge Reactor Design Limited. Crystallisation Process and Apparatus. International Patent, WO 2011/051728 A1, 5 May 2011.
8. Saleemi, A.N.; Rielly, C.D.; Nagy, Z.K. Monitoring of the combined cooling and antisolvent crystallisation of mixtures of aminobenzoic acid isomers using ATR-UV/vis spectroscopy and FBRM. *Chem. Eng. Sci.* **2012**, *77*, 122–129.
9. Quon, J.L.; Zhang, H.; Alvarez, A.; Evans, J.; Myerson, A.S.; Trout, B.L. Continuous Crystallization of Aliskiren Hemifumarate. *Cryst. Growth Des.* **2012**, *12*, 3036–3044.
10. Nagy, Z.K.; Mitsuko, F.; Woo, X.Y.; Braatz, R.D. Determination of the Kinetic Parameters for the Crystallzation of Paracetamol from Water Using Metastable Zone Width Experiments. *Ind. Eng. Chem. Res.* **2008**, *47*, 1245–1252.
11. Nyvlt, J.; Sohnel, O.; Matuchova, M.; Brout, M. *The Kinetics of Industrial Crystalisation*; Elsevier: Amsterdam, The Netherlands, 1985.
12. ur Rehman, A.; Helliwell, M.; Ali, S.; Shahzadi, S. 4-chloro-3,5-dinitrobenzoic acid. *Acta Crystallogr. Sect. E Struct. Rep. Online* **2007**, *63*, O1743–O1744.
13. *ReactArray Solo (Software)*, version 0.9.0.0; Anachem Ltd.: Luton, UK, 2005.
14. Sheldrick, G.M. A short history of SHELX. *Acta Crystallogr. Sect. A* **2008**, *64*, 112–122.
15. Farrugia, L.J. WinGX Suite for Single Crystal Small Molecule Crystallography. *J. Appl. Cryst.* **1999**, *32*, 837–838.
16. Farrugia, L.J. WinGX and ORTEP for Windows: An update. *J. Appl. Crystallogr.* **2012**, *45*, 849–854.
17. *Advantage (Software)*, version 5.5.3; TA Instruments: New Castle, DE, USA, 2013.
18. *CrystalClear (Software)*, version 1.0.1.614; Avantium Technologies BV: Amsterdam, The Netherlands, 2013.
19. Habgood, M.; Deij, M.A.; Mazurek, J.; Price, S.L.; ter Horst, J.H. Carbamazepine Co-crystallization with Pyridine Carboxamides: Rationalization by Complementary Phase Diagrams and Crystal Energy Landscapes. *Cryst. Growth Des.* **2010**, *10*, 903–912.

20. Kulkarni, S.A.; Kadam, S.S.; Meekes, H.; Stankiewicz, A.I.; ter Horst, J.H. Crystal Nucleation Kinetics from Induction Times and Metastable Zone Widths. *Cryst. Growth Des.* **2013**, *13*, 2435–2440.
21. ter Horst, J.H. Industrial Crystallization: Fundamental Understanding for Challenges Ahead. *Chem. Eng. Technol.* **2012**, *35*, 965–965.